

Disorder-Induced Multiple Transition involving \mathbb{Z}_2 Topological Insulator

Ai Yamakage*, Kentaro Nomura¹, Ken-Ichiro Imura², and Yoshio Kuramoto

Department of Physics, Tohoku University, Sendai 980-8578, Japan

¹*Correlated Electron Research Group (CERG), RIKEN-ASI, Wako 351-0198, Japan*

²*Department of Quantum Matter, AdSM, Hiroshima University, Higashi-Hiroshima 739-8530, Japan*

Effects of disorder on two-dimensional \mathbb{Z}_2 topological insulator are studied numerically by the transfer matrix method. Based on the scaling analysis, the phase diagram is derived for a model of HgTe quantum well as a function of disorder strength and magnitude of the energy gap. In the presence of s_z non-conserving spin-orbit coupling, a finite metallic region is found that partitions the two topologically distinct insulating phases. As disorder increases, a narrow-gap topologically trivial insulator undergoes a series of transitions; first to metal, second to topological insulator, third to metal, and finally back to trivial insulator. We show that this multiple transition is a consequence of two disorder effects; renormalization of the band gap, and Anderson localization. The metallic region found in the scaling analysis corresponds roughly to the region of finite density of states at the Fermi level evaluated in the self-consistent Born approximation.

KEYWORDS: \mathbb{Z}_2 topological insulator, HgTe, disorder, phase diagram, density of states, transfer matrix, self-consistent Born approximation

Topological insulator is a distinct type of insulator, showing a metallic surface state. During the last few years an increasing attention has been on its \mathbb{Z}_2 version¹⁻³⁾ which realizes without an external magnetic field and preserves time-reversal symmetry. This is contrasting to a more prototypical integer quantum Hall insulator. Another twist motivating the present study is a recent proposal on the concept of so-called “topological Anderson insulator” (TAI).⁴⁻⁶⁾ which extends the limit of topological distinction beyond that of band insulator.

In two spatial dimensions (2D) disorder plays a fundamental role in electronic transport. This paper deals with a 2D version of the \mathbb{Z}_2 topological insulator (\mathbb{Z}_2 TI), a variant of the model proposed by Bernevig, Hughes, and Zhang; hereafter referred to as BHZ.⁷⁾ The BHZ model has been proposed to describe a \mathbb{Z}_2 TI implemented in HgTe/CdTe superstructure.^{8,9)} An important element added in this study to the BHZ model is a Rashba-type spin-orbit coupling (SOC), which breaks spin-axial symmetry along z -axis inherent to the original version of BHZ model. This s_z non-conserving SOC changes the topological invariant characterizing insulator from \mathbb{Z} to \mathbb{Z}_2 .^{10,11)}

Effects of disorder on topological insulators have been extensively studied.^{4-6,12-18)} Directly relevant to this Letter are refs.¹²⁻¹⁴⁾ which have treated the s_z non-conserving cases of \mathbb{Z}_2 TI, and refs.⁴⁻⁶⁾ dealing with TAI. The basic viewpoint on TAI on which we are based is due to ref.⁶⁾ i.e., spin-independent potential disorder brings about renormalization of the gap, both its magnitude and sign, allowing for conversion of an ordinary band insulator to a topologically non-trivial one. On the other hand, a metallic behavior induced by disorder is also expected in the s_z non-conserving system we study. Since the existing studies on TAI dealt with the s_z conserving case,

there was no discussion about how such metallic conduction combines with the renormalization of band gap and localization effect to determine the phase diagram of disordered BHZ model with s_z non-conserving SOC. This paper takes full account of such Rashba-type spin-flip terms incorporated in the BHZ model and deduces a phase diagram of the disordered and disorder-induced \mathbb{Z}_2 TI. We demonstrate that disordered BHZ model shows as many as four transitions for a given value of trivial band gap as a function of disorder. As disorder increases, a narrow-gap topologically trivial insulator first turns to a metal, second to a topological insulator, third again to a metal, and finally back to the trivial insulator. Occurrence of such “multiple transition” intervened by a finite metallic region is a distinct property, providing us also with a useful point of view on the understanding of TAI.

We consider a tight-binding version of the BHZ model on 2D square lattice. We add Rashba-type SOC in order to generalize to include the electric field perpendicular to surface, which is induced by structural inversion asymmetry of the quantum well or gate electrode. Without disorder, the Hamiltonian becomes block diagonal in momentum space and reduces to the following 4×4 matrices,^{7,9,19,20)}

$$\mathcal{H}(\mathbf{k}) = \begin{bmatrix} h(\mathbf{k}) & \Gamma(\mathbf{k}) \\ \Gamma(\mathbf{k})^\dagger & h^*(-\mathbf{k}) \end{bmatrix}. \quad (1)$$

The first (last) rows/columns correspond to real spin \uparrow (\downarrow), i.e., $s_z = \pm 1$. The 2×2 matrix $\Gamma(\mathbf{k})$ represents Rashba SOC, the explicit form of which will be determined by symmetry arguments. The diagonal blocks, $h(\mathbf{k})$ and its Kramers’ partner $h^*(-\mathbf{k})$, are of 2D Dirac form: e.g., $h(\mathbf{k}) = \mathbf{d}(\mathbf{k}) \cdot \boldsymbol{\sigma}$, where

$$\mathbf{d}(\mathbf{k}) = (A \sin k_x, A \sin k_y, \Delta - 2B(2 - \cos k_x - \cos k_y)).$$

$\boldsymbol{\sigma}$ is another set of Pauli matrices (than the real spin

*E-mail address: ai@cmtpt.phys.tohoku.ac.jp

$\mathbf{s} = (s_x, s_y, s_z)$, representing an orbital pseudo-spin. The parameter Δ , which is associated with the band gap, can be tuned by varying the thickness of HgTe layer. Then nontrivial phase with \mathbb{Z}_2 topological invariant $\nu = 1$ realizes when $0 < \Delta/B < 4$ and $4 < \Delta/B < 8$, whereas trivial phase with $\nu = 0$ corresponds to $\Delta/B < 0$ and $\Delta/B > 8$.

In the presence of a random potential, the total Hamiltonian is defined only in real space,

$$H = \sum_{\mathbf{r}} \left[c_{\mathbf{r}}^{\dagger} \epsilon_{\mathbf{r}} c_{\mathbf{r}} + \left(c_{\mathbf{r}+\mathbf{a}}^{\dagger} t_x c_{\mathbf{r}} + c_{\mathbf{r}+\mathbf{b}}^{\dagger} t_y c_{\mathbf{r}} + h.c. \right) \right], \quad (2)$$

where $\mathbf{r} = (I, J)$ represents a site on 2D square lattice, and $\mathbf{a} = (1, 0)$ and $\mathbf{b} = (0, 1)$ are primitive lattice vectors with the lattice constant set to unity. Explicit form of the hopping matrices t_x and t_y are determined as follows. We take the Rashba-type interaction, $H_{\text{R}} \propto (\mathbf{p} \times \mathbf{s})_z = p_x s_y - p_y s_x$, and adapt it to the BHZ model. The two components of the orbital pseudo-spin consist of Γ_6 orbital with the total angular momentum $j = 1/2$, and one of Γ_8 orbitals with $j = 3/2$ and $j_z = \pm 3/2$. The form of H_{R} is constrained due to various symmetry requirements. First, notice that hopping matrix elements transform under π rotation with respect to the y -axis as,

$$\begin{aligned} \alpha/2 &\equiv \langle \mathbf{a}, j_z | H_{\text{R}} | \mathbf{0}, -j_z \rangle = -\langle -\mathbf{a}, -j_z | (-H_{\text{R}}) | \mathbf{0}, j_z \rangle \\ &= \langle \mathbf{0}, j_z | H_{\text{R}} | -\mathbf{a}, -j_z \rangle^*. \end{aligned} \quad (3)$$

Here, particle-hole symmetry is assumed, implying that the matrix elements considered are independent of j_z . Combined with translational invariance, eq. (3) guarantees that α is *real*. Second, invariance under $\pi/2$ rotation with respect to the z -axis requires, on the other hand,

$$\begin{aligned} \langle \mathbf{a}, j_z | H_{\text{R}} | \mathbf{0}, -j_z \rangle &= \pm i \langle \mathbf{b}, j_z | H_{\text{R}} | \mathbf{0}, -j_z \rangle \\ &= -\langle -\mathbf{a}, j_z | H_{\text{R}} | \mathbf{0}, -j_z \rangle, \end{aligned} \quad (4)$$

where a positive (negative) sign corresponds to $j_z = \pm 1/2$ ($\pm 3/2$). Note that $\pi/2$ rotation gives rise to a factor, $\exp(ij_z\pi) = \pm i$. By combining eqs. (3) and (4), hopping matrices t_x and t_y are determined as,

$$t_x = B\sigma_z - i\frac{A}{2}\sigma_x s_z + i\frac{\alpha}{2}s_y, \quad (5)$$

$$t_y = B\sigma_z + i\frac{A}{2}\sigma_y - i\frac{\alpha}{2}\sigma_z s_x. \quad (6)$$

Thus off-diagonal coupling in eq. (1) has been determined as,

$$\Gamma(\mathbf{k}) = i\alpha \text{diag} [\sin k_x - i \sin k_y, \sin k_x + i \sin k_y]. \quad (7)$$

Terms connecting $j_z = \pm 1/2$ and $j_z = \mp 3/2$ states are neglected, for simplicity.

For the impurity potential, we take a site-diagonal form. The local energy $\epsilon_{\mathbf{r}}$ at site \mathbf{r} is given by

$$\epsilon_{\mathbf{r}} = (\Delta - 4B)\sigma_z \otimes \mathbb{I} + \text{diag} \left[W_{\mathbf{r}}^{(s)}, W_{\mathbf{r}}^{(p)} \right] \otimes \mathbb{I} \quad (8)$$

where \mathbb{I} is 2×2 identity matrix in spin space, and strength of non-magnetic disorder is specified by $W_{\mathbf{r}}^{(s)}$ and $W_{\mathbf{r}}^{(p)}$ for Γ_6 - and Γ_8 -type orbitals, respectively.⁷⁾ It is assumed

that each impurity potential obeys uniform distribution in the period: $[-W/2, W/2]$.

We have performed extensive numerical study on the localization length λ_L using the transfer matrix method.²¹⁾ For a given set of parameters (Δ, W) , the localization length λ_L is estimated by varying the system size L . If λ_L/L decreases (increases) with increasing L , the system is judged to be insulating (metallic). Hereafter, we concentrate on the case of $E = 0$, where the Fermi level is located in the middle of band gap. The other parameters are fixed as $A = B = 1$. We identify the localization characteristics from scaling behavior of the localization length λ_L , and determine the phase boundaries between metallic and insulating regions.

Figure 1 shows representative data for different size of the system in the presence of s_z non-conserving SOC with $\alpha = 0.5$. In the upper panel, λ_L/L is plotted as a function of W with $\Delta = -1$ fixed. At each value of W , λ_L is evaluated for systems of different circumference L . It is clear that there are two values of W where λ_L/L does not depend on L . This indicates a critical point that separates metallic and insulating regimes. In contrast with ordinary phase transitions, the critical point is meaningful only at zero temperature, as an example of the quantum phase transition. As W increases from zero, the system becomes metallic at $W = W_1 \sim 7$ up to $W_2 \sim 9.5$. When W is further increased, λ_L/L shows again a monotonic decrease as a function of L . Namely we observe a *reentrant* behavior: localized \rightarrow metallic \rightarrow localized, with increasing W . The emergence of metallic state by the s_z non-conserving SOC has already been studied by ref.12 for the Kane-Mele model of graphene, which belongs to a topological insulator in the clean limit. In our case, however, the value $\Delta = -1$ means that the system is the trivial insulator in the clean limit. Namely, in contradiction to naive intuition, the disorder first converts insulator to metal, and then back to insulator.

The lower panel of Fig. 1 shows λ_L/L as a function of Δ with fixed $W = 6$. At each value of Δ , λ_L/L is evaluated for systems of different circumference L . Overall behavior of λ_L/L looks similar to that of the upper panel. Namely, as Δ increases, the system evolves as: localized \rightarrow metallic \rightarrow localized. Note that the first insulating phase: $\Delta < \Delta_1 \sim -0.8$ is of trivial nature ($\nu = 0$), whereas the second one with $\Delta > \Delta_2 \sim -0.5$ is \mathbb{Z}_2 nontrivial ($\nu = 1$). These different kinds are separated by a finite metallic region: $\Delta_1 < \Delta < \Delta_2$. The second insulating phase with \mathbb{Z}_2 -number $\nu = 1$ starts already at a negative value: $\Delta_{c_2} \sim -0.5$. This result demonstrates that a \mathbb{Z}_2 topological insulator can be induced by introducing non-magnetic disorder to a clean trivial insulator. In recent literature, similar disorder-induced \mathbb{Z}_2 -nontrivial phase has been discussed,⁴⁻⁶⁾ but without the intervening metallic region.

By repeating such analysis for different values of Δ and W , and identifying critical points, we obtain the phase diagram of the system at the ground state. In the clean limit, the nontrivial phase appears in the region $0 < \Delta < 4$ and $4 < \Delta < 8$. Only the region with $\Delta < 4$ is shown in Fig.2 since the phase diagram is reflection

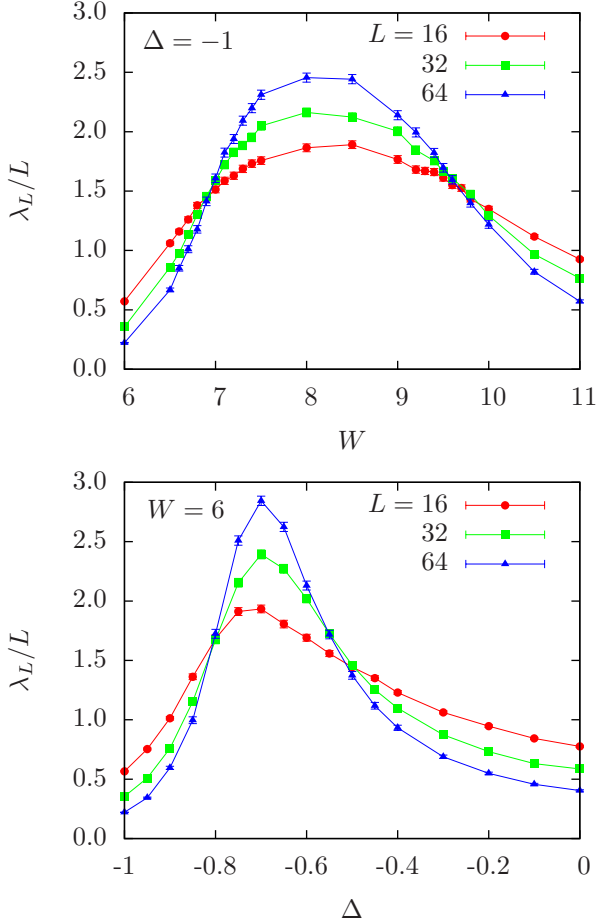


Fig. 1. (color online) Scaling behavior of λ_L as a function of W (upper panel) and Δ (lower panel). In the upper panel, the system with $\Delta = -1$ is topologically trivial in the clean limit. The lower panel shows the behavior of “ \mathbb{Z}_2 topological Anderson insulator”,⁴⁻⁶ since the region $\Delta > -0.5$ is made topologically nontrivial by the effect of W .

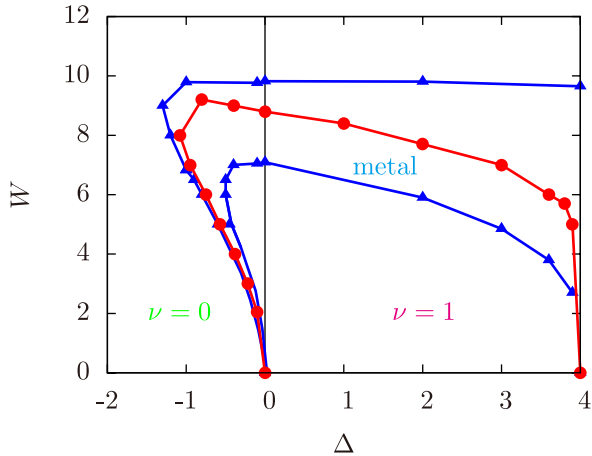


Fig. 2. (color online) Phase diagram of disordered BHZ model in the presence ($\alpha = 0.5$, blue triangles) and absence ($\alpha = 0$, red circles) of s_z non-conserving SOC. Lines connecting the data points are guide to eyes.

symmetric about $\Delta = 4$. The particle-hole symmetry is responsible for this property. For comparison, we also show the s_z conserving case with $\alpha = 0$. In this case the system is always insulating except along the transition line indicated by (red) circles.

Let us focus on the s_z non-conserving ($\alpha \neq 0$) SOC effects. The triangle symbols (blue) show the transition points between metallic and insulating phases. It is clear that the metallic region emerges in the vicinity of the transition line at $\alpha = 0$. Consequently, the two topologically distinct insulating phases are always separated by a metallic region of finite width. Furthermore, $\nu = 1$ phase is extended toward $\Delta < 0$ by finite disorder. Unfortunately, in the weak-disordered region below $W \sim 4$ with $\alpha = 0.5$, we have been unable to determine the transition point from the data up to 64 sites due to strong finite-size effect. The transition can occur, on the other hand, only at $\Delta = 0$ in the clean limit, and the transition line should be continuously connected. Therefore, with decreasing W , it is reasonable to assume that the metallic corridor persists and converges to the point $\Delta = 0$. As a result, increasing the strength of disorder W , multiple transition occurs in such a way as:

- (i) \mathbb{Z}_2 -nontrivial \rightarrow metallic \rightarrow \mathbb{Z}_2 -trivial for positive Δ ;
- (ii) \mathbb{Z}_2 -trivial \rightarrow metallic \rightarrow \mathbb{Z}_2 -nontrivial \rightarrow metallic \rightarrow \mathbb{Z}_2 -trivial for $-0.5 \lesssim \Delta < 0$.

These multiple transition are to be contrasted with the case $\alpha = 0$ where intervening metallic phases are absent.

It is natural to ask the origin of the reentrant behavior with negative Δ . In order to answer the question, we now turn to the density of states $\rho(E)$ of the system. Let us first study how the region of nonzero $\rho(0)$ is correlated to the region of metallic conduction. We follow the previous study⁶ for the s_z conserving case ($\alpha = 0$), to employ the self-consistent Born approximation (SCBA). Note that interference of electronic wave functions, which is crucial for the Anderson localization, is beyond the scope of the SCBA. However, the SCBA does describe disorder-induced renormalization of Δ , whose sign distinguishes whether the system is topologically trivial or not.

Effects of disorder are taken into account in the SCBA as the self-energy $\Sigma(E)$ of the Green function $G(\mathbf{k}, E)$, which is the 4×4 matrix in our case. We decompose the self-energy matrix as $\Sigma = \Sigma_0 + \Sigma_z \sigma_z$. Note that the self energy is a scalar in the (real) spin space due to time-reversal symmetry. The renormalization of parameters occurs as

$$\Delta \rightarrow \tilde{\Delta}(E) = \Delta + \text{Re} \Sigma_z(E), \quad (9)$$

$$E \rightarrow \tilde{E}(E) = E - \text{Re} \Sigma_0(E), \quad (10)$$

where $|\tilde{\Delta}|$ represents the renormalized energy gap, and \tilde{E} is the shift of the energy. The SCBA gives the following self-consistency equation:

$$\Sigma(E) = \frac{W^2}{12} \int \frac{d^2 k}{(2\pi)^2} \langle G(\mathbf{k}, E) \rangle, \quad (11)$$

where $\langle G(\mathbf{k}, E) \rangle = \langle (E - \mathcal{H}(\mathbf{k}) - \Sigma(E))^{-1} \rangle$ is the disorder-averaged Green function. Because of particle-hole sym-

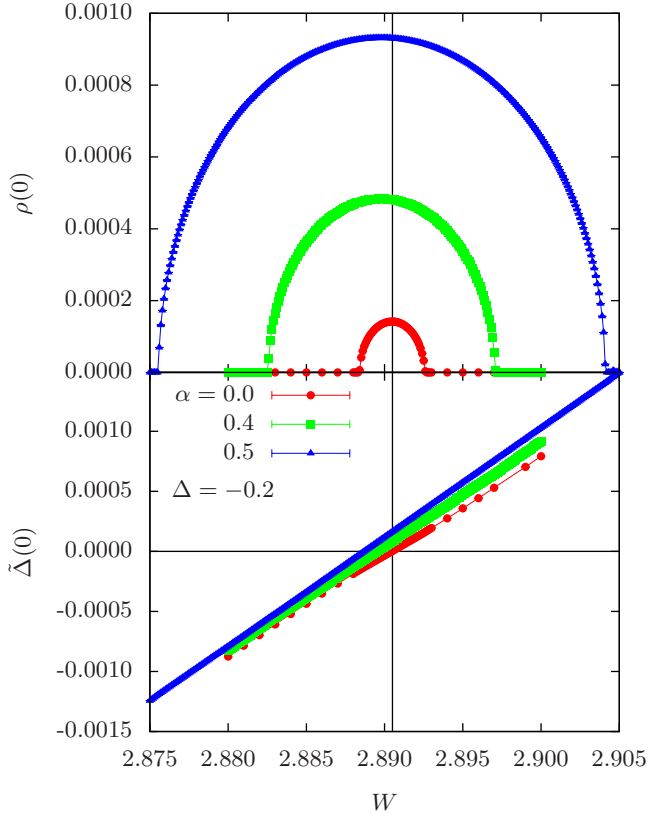


Fig. 3. (color online) Density of states $\rho(0)$ (upper part) and renormalized mass $\tilde{\Delta}(0)$ (lower part) as a function of W with fixed $\Delta = -0.2$ for different values of α . In the SCBA, $\tilde{\Delta}$'s for various α vanish commonly at $W \sim 2.89$, which corresponds roughly to the peak of $\rho(0)$.

metry, $\text{Re } \Sigma_0(0)$ and $\text{Im } \Sigma_z(0)$ vanish. Hence the Fermi level at $E = 0$ is not shifted. The density of states is given by

$$\rho(E) = -\frac{1}{\pi} \text{Im tr } G(E) = -\frac{24}{\pi} \text{Im } \Sigma_0(E). \quad (12)$$

We solve Eq. (11) and derive $\text{Im } \Sigma_0(0)$ and $\text{Re } \Sigma_z(0)$. Near the metal-insulator transition, $\text{Im } \Sigma_z(0)$ is small and converges only slowly in the iterative method. Therefore we apply a root finding procedure called Steffensen's method only for $\text{Im } \Sigma_0(0)$ in order to accelerate the convergence.

Figure 3 shows the density of states $\rho(0)$ (upper part) together with the renormalized gap $\tilde{\Delta}(0) = \Delta + \Sigma_z(0)$ (lower part) at the particle-hole symmetric point $E = 0$. Results at fixed $\Delta = -0.2$ but with different values of α is given for comparison. In the upper part $\rho(0)$ is plotted as a function of W , which shows in all cases a finite range of finite $\rho(0)$. According to the SCBA, the density of states $\rho(0)$ vanishes outside this range. The change of $\rho(0)$ as a function of W with decreasing α seems continuous down to the limit $\alpha = 0$. Both the width and the magnitude of the region with finite $\rho(0)$ decreases with decreasing α , but remains finite at $\alpha = 0$.

The lower part in Fig. 3 shows that $\tilde{\Delta}(0)$ changes sign around $W \sim 2.89$, which corresponds roughly to the peak of $\rho(0)$. Note that the bare value in the present case is $\Delta = -0.2$, which corresponds to the trivial insulator with

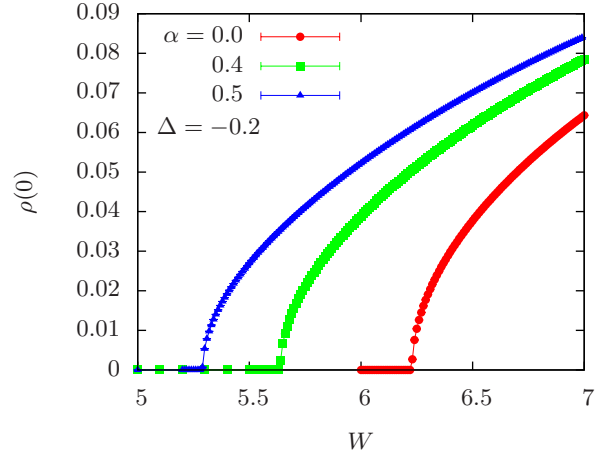


Fig. 4. (color line) Density of states in the strongly disordered region for the same parameters as in Fig. 3.

$\nu = 0$. Thus we find that the disorder drives the system into topologically nontrivial regime by renormalizing $\tilde{\Delta}(0)$ to a positive value. The change of $\tilde{\Delta}(0)$ depends only slightly on α as shown in Fig. 3. Correspondingly, $\rho(0)$ becomes finite in a finite range of W on both sides of the band inversion point ($\tilde{\Delta} = 0$).

As W is further increased, $\rho(0)$ vanishes and stays null until the second onset of the topological transition as shown in Fig. 4. Finite value for $\rho(0)$ resumes slightly before the entrance to the metallic phase shown in Fig. 2. We have found that, after the second onset, $\rho(0)$ never decreases but continues to grow with increasing W . In other words, the end of the metallic phase around $W = 10$ shown in Fig. 2 cannot be reproduced by the SCBA. Although the density of states is finite for large W , the wave function is actually Anderson-localized. The SCBA cannot describe this localization property. Hence, it will safely be said that the reentrant behavior of the phase transition is partly understood by the renormalization of $\tilde{\Delta}(0)$ and the onset of $\rho(0)$ within the SCBA, especially in the range of small W .

In conclusion, we have derived the phase diagram of disordered BHZ model in the presence of s_z non-conserving SOC. As a crucial effect of s_z non-conserving SOC, we have demonstrated that metallic state intrudes each transition. While TAI is realized as a distinct state in (W, E) -space,⁴ it is connected continuously to clean topological insulator in (Δ, W) -space. Furthermore, the origin of reentrant behavior is investigated in terms of the SCBA. As in the case of $\alpha = 0$ studied earlier,⁶ we have found for $\alpha \neq 0$ that the disorder drives originally negative Δ to positive. This change of sign causes the topological transition induced by disorder. However, as an important difference from the previous study, we find that metallic state always accompanies the topological transitions in the phase diagram. Actual 2D \mathbb{Z}_2 TI systems such as HgTe quantum wells have a sizable s_z non-conserving SOC, which can be tuned continuously by gate voltage. We hope that our results encourage experimental detection of (multiple) topological transitions with metallic intruders.

AY acknowledges Grant-in-Aid for JSPS Fellows under Grants No. 08J56061. KN and KI are supported by Grant-in-Aid for Young Scientists (B) under Grants Nos. 20740167 (KN) and 19740189 (KI). KN is also supported by FIRST program (JSPS). We acknowledge C. Brüne and E. Prodan for helpful discussions and correspondences.

- 1) J. E. Moore: *Nature* **464** (2010) 194.
- 2) M. Z. Hasan and C. L. Kane: *Rev. Mod. Phys.* **82** (2010) 3045.
- 3) X.-L. Qi and S.-C. Zhang: arXiv:1008.2026 (2010).
- 4) J. Li, R.-L. Chu, J. K. Jain, and S.-Q. Shen: *Phys. Rev. Lett.* **102** (2009) 136806.
- 5) H. Jiang, L. Wang, Q.-F. Sun, and X. C. Xie: *Phys. Rev. B* **80** (2009) 165316.
- 6) C. W. Groth, M. Wimmer, A. R. Akhmerov, J. Tworzydło, and C. W. J. Beenakker: *Phys. Rev. Lett.* **103** (2009) 196805.
- 7) B. A. Bernevig, T. L. Hughes, and S.-C. Zhang: *Science* **314** (2006) 1757.
- 8) M. König, S. Wiedmann, C. Brüne, A. Roth, H. Buhmann, L. W. Molenkamp, X.-L. Qi, and S.-C. Zhang: *Science* **318** (2007) 766.
- 9) M. König, H. Buhmann, L. W. Molenkamp, T. Hughes, C.-X. Liu, X.-L. Qi, and S.-C. Zhang: *J. Phys. Soc. Jpn* **77** (2008) 031007.
- 10) C. L. Kane and E. J. Mele: *Phys. Rev. Lett.* **95** (2005) 226801.
- 11) C. L. Kane and E. J. Mele: *Phys. Rev. Lett.* **95** (2005) 146802.
- 12) M. Onoda, Y. Avishai, and N. Nagaosa: *Phys. Rev. Lett.* **98** (2007) 076802.
- 13) H. Obuse, A. Furusaki, S. Ryu, and C. Mudry: *Phys. Rev. B* **76** (2007) 075301.
- 14) K. Imura, Y. Kuramoto, and K. Nomura: *Eur. Phys. Lett.* **89** (2010) 17009.
- 15) R. Shindou and S. Murakami: *Phys. Rev. B* **79** (2009) 045321.
- 16) H.-M. Guo, G. Rosenberg, G. Refael, and M. Franz: *Phys. Rev. Lett.* **105** (2010) 216601.
- 17) E. Prodan: arXiv:1010.0595 (2010).
- 18) P. Goswami and S. Chakravarty: arXiv:1101.2210 (2011).
- 19) J. Maciejko, X.-L. Qi, and S.-C. Zhang: *Phys. Rev. B* **82** (2010) 155310.
- 20) D. G. Rothe, R. W. Reinthaler, C.-X. Liu, L. W. Molenkamp, S.-C. Zhang, and E. M. Hankiewicz: *New J. Phys.* **12** (2010) 065012.
- 21) A. MacKinnon and B. Kramer: *Z. Phys. B* **53** (1983) 1.